Journal of Power Sources 294 (2015) 333–338

Contents lists available at ScienceDirect

Journal of Power Sources

journal homepage: www.elsevier.com/locate/jpowsour

High performance electrodes in vanadium redox flow batteries through oxygen-enriched thermal activation

Alan M. Pezeshki [a, b, c], Jason T. Clement [d], Gabriel M. Veith [c], Thomas A. Zawodzinski [a, c], Matthew M. Mench [d, e, *]

[a] Department of Chemical and Biomolecular Engineering, University of Tennessee, Knoxville, TN 37996, USA
[b] Bredesen Center for Interdisciplinary Research and Graduate Education, University of Tennessee, Knoxville, TN 37996, USA
[c] Materials Science and Technology Division, Oak Ridge National Laboratory, Oak Ridge, TN 37831, USA
[d] Department of Mechanical, Aerospace, and Biomedical Engineering, University of Tennessee, Knoxville, TN 37996, USA
[e] Energy and Transportation Science Division, Oak Ridge National Laboratory, Oak Ridge, TN 37831, USA

HIGHLIGHTS

- Thermal activation of carbon paper electrodes enhances VRFB kinetic performance.
- Large increase in surface area is responsible for improved kinetic performance.
- Significant improvement in depth of charge is achieved.
- Charge/discharge cycling efficiency of 76% at 200 mA cm^{-2} is realized.

ARTICLE INFO

Article history:
Received 20 February 2015
Received in revised form
10 April 2015
Accepted 30 May 2015
Available online xxx

Keywords:
Vanadium redox flow battery
Carbon paper
Kinetics
Surface area
Thermal activation
Electrode

ABSTRACT

The roundtrip electrochemical energy efficiency is improved from 63% to 76% at a current density of 200 mA cm^{-2} in an all-vanadium redox flow battery (VRFB) by utilizing modified carbon paper electrodes in the high-performance no-gap design. Heat treatment of the carbon paper electrodes in a 42% oxygen/58% nitrogen atmosphere increases the electrochemically wetted surface area from 0.24 to 51.22 m^2 g^{-1}, resulting in a 100–140 mV decrease in activation overpotential at operationally relevant current densities. An enriched oxygen environment decreases the amount of treatment time required to achieve high surface area. The increased efficiency and greater depth of discharge doubles the total usable energy stored in a fixed amount of electrolyte during operation at 200 mA cm^{-2}.

1. Introduction

Redox flow batteries, initially researched by NASA in the 1970s, have risen to prominence as an energy storage technology and are an important factor in enabling wide-scale implementation of intermittent renewable energy sources on the grid [1]. Among them, the all-vanadium redox flow battery (VRFB) has drawn considerable attention; however, system costs are a barrier to commercialization. The stack is estimated to account for roughly 30% of the total cost, and the vanadium-based electrolyte accounts for nearly 40% given conventional system operating parameters and design [2]. Recent studies have focused on improving electrode and membrane performance to increase power density and therefore decrease stack-associated costs [3–7]. These advancements also improve efficiency, which reduces electrolyte cost since more energy can be extracted per charged vanadium ion.

Activation overpotential as a result of sluggish electrode kinetics is one cause of efficiency loss in electrochemical systems. Electrode kinetic overpotential is a function of electrode surface area and surface chemistry [8,9]. Many studies have attempted to modify carbon or graphite felt surface chemistry through chemical [10–12]

* Corresponding author. 410 Dougherty Eng. Bldg. University of Tennessee Knoxville, TN 37996-2210, USA.
E-mail address: mmench@utk.edu (M.M. Mench).

http://dx.doi.org/10.1016/j.jpowsour.2015.05.118
0378-7753/

and thermal treatments [12–14]. In these investigations, increased activity of the electrode surface is generally attributed to enhanced oxygen content on the surface. However, the connection between oxygen content and electrode activity has not been conclusively verified.

Thermal treatments on graphite felts were first pioneered in VRFB systems by Sun and Skyllas-Kazacos [13]. In the current study, carbon paper electrodes were thermally treated under varied oxygen concentrations and then used in the high power density no-gap architecture [6]. This work demonstrates performance gains and associated system-level benefits that can be achieved by using enhanced carbon paper electrodes in a favorable architecture. The use of an enriched oxygen environment during treatment decreases the amount of time required for heat treatment, resulting in energy and cost savings during processing. Initial characterization results indicate that the large increase in surface area was responsible for the enhanced kinetic performance, rather than the addition of oxygen functionalities, as previous authors have suggested [10–14]. This implies that electrode modification studies must account for the change in surface area to complement analysis of the surface chemistry when attempting to explain any apparent change in electrode kinetics.

2. Experimental methods

2.1. Electrode preparation

Untreated SGL10AA carbon paper (SGL Group) was used as the baseline electrode material. Nine sets of the 10AA electrodes were heat treated in a tube furnace at 400 °C with oxygen concentrations of 0% (nitrogen), 21% (air), and 42% (enriched) balanced by nitrogen (Airgas) for 15, 30, and 45 h for each oxygen concentration. Prior to heat treatment, the electrodes were purged in the furnace with the treatment gas for 2 h. Selected electrodes were characterized to determine oxygen content, surface area, and wetted surface area with a PHI 3056 X-ray photoelectron spectrometer (XPS) with an Al K_α X-ray source (1486.6 eV) at 350 W, an Autosorb-iQ surface area analyzer (BET method), and electrochemical impedance spectroscopy, respectively [15]. Mass loss was determined by weighing samples before and after heat treatment.

2.2. Cell architecture

Single-cell flow batteries with 5 cm^2 of geometric active area were constructed with a serpentine flow field using the no-gap architecture [6]. Three layers of carbon paper compressed to ca. 70% of their original thickness were used in both sides of the cell. A Nafion® 117 membrane (DuPont) was utilized to maximize coulombic efficiency. For all testing, a flow rate of 90 mL min^{-1} was provided by a dual-channel peristaltic pump (Cole–Parmer). Cell temperature was maintained at 30 °C.

2.3. Electrolyte solution

Electrolyte solutions consisting of 1 M vanadium ions in 5 M sulfuric acid were prepared from vanadium (IV) sulfate oxide hydrate (Alfa Aesar, 99.9%) and sulfuric acid (Alfa Aesar, ACS grade) in deionized water. Initial charging was performed with 100 mL catholyte and 50 mL anolyte. Upon reaching ca. 100% state of charge (SoC), one half of the catholyte solution was discarded to obtain a 1:1 ratio of charged catholyte and anolyte solutions. A nitrogen purge (Airgas, UHP) was used over both tanks of electrolyte to prevent oxidation of the vanadium species.

2.4. Electrochemical characterization

Polarization curves were obtained with alternating 30 s galvanostatic discharge and open-circuit steps with no recharge, resulting in a continuous decrease in SoC over the course of the curve. High-frequency resistance (HFR) measurements were taken during discharge steps to *iR*-correct the polarization curves. Two cycles at both 100 mA cm^{-2} and 200 mA cm^{-2} were carried out with the same electrolyte solution used for the polarization curves. Cutoff voltages of 1.7 and 0.6 V were used upon charge and discharge, respectively. HFR measurements were also taken during cycling and used to *iR*-correct the charge and discharge profiles. Electrochemical measurement and control and temperature control were carried out with a Scribner Associates 857 Redox Test System potentiostat.

3. Results and discussion

3.1. Polarization curves

With the passage of current, electrochemical systems deviate from their thermodynamic cell potential due to activation/kinetic, ohmic, and concentration polarizations. Polarization curves are a useful tool for resolving these sources of overpotential [16]. In this work, polarization curves were *iR*-corrected to remove the ohmic losses from the membrane, leaving ohmic losses in the liquid electrolyte and activation and concentration polarizations. While these contributors to polarization appear over all current densities, the activation overpotential dominates at lower current densities [17]. Given that there was no significant difference between polarization curves with and without recharge between discharge steps for low current densities (0–0.5 A cm^{-2}), the concentration polarization is negligible in the low current density regime. Ohmic losses in the liquid electrolyte were assumed to be similar between different cell builds and are not discussed in the remainder of this work.

Treatment in nitrogen (0% oxygen) provides a moderate improvement in cell performance, while treatments in air (21% oxygen) and enriched (42%) oxygen provide a more marked improvement, as shown by the *iR*-corrected curves with the 15 h treated electrodes in Fig. 1(a). Similar trends were observed for both 30 and 45 h treated carbon papers. Fig. 1(b) shows the difference in *iR*-corrected voltage between each of the treated and untreated electrodes. The air and enriched oxygen treatments resulted in improvements of 100 mV over untreated carbon paper at a current density of 100 mA cm^{-2} that asymptote to 140 mV at 0.5 A cm^{-2}. The pure nitrogen treatment showed a more modest boost of 40 mV that does not increase with current density beyond 40 mA cm^{-2}. Sharp gains in the low current density region of the polarization curve (0–0.5 A cm^{-2}) with gains that level off at higher current densities (>0.5 A cm^{-2}) indicate an improvement in the kinetic performance of the vanadium redox reactions on the electrode surface.

3.2. Electrode characterization

Both surface area and chemistry have an impact on reaction rates. The surface chemistry, probed with XPS, showed a small increase in oxygen content on the electrode, from 1% untreated to 2% with the enriched oxygen treated electrode. This change is much smaller than the increase from 4% to 20% observed by Sun and Skyllas-Kazacos on heat treated carbon felt [13]; however, carbon paper is a different material than felt and may be less susceptible to oxygen functionalization. The BET surface area of the 42% oxygen treated material was 21.0 m^2 g^{-1}, a significant gain over the

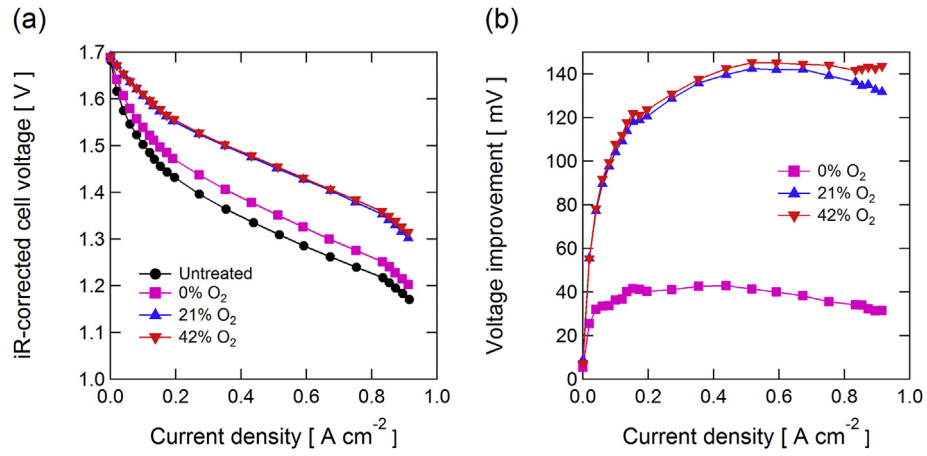

Fig. 1. (a) *iR*-corrected polarization curves for untreated carbon paper and those treated for 15 h in 0%, 21%, and 42% oxygen environments and (b) *iR*-corrected voltage improvement of each heat treatment relative to untreated carbon paper.

1.0 $m^2\ g^{-1}$ [15] for the untreated material. This increase in surface area is likely a roughening of the carbon fiber surface that is not visible by SEM; Lee and Kang confirmed by atomic force microscopy that heat treating PAN-based carbon fibers introduces micropores in the carbon fiber structure [18]. Because BET surface area measurements may be limited by the ability of nitrogen physisorption to probe extremely small pores [19], the double-layer capacitance was also measured and used to estimate the surface area. This method provides a more accurate measure of the electrochemically active wetted surface area. The capacitance measured by electrochemical impedance spectroscopy indicated the wetted surface area increased from 0.24 $m^2\ g^{-1}$ untreated [15] to 39.10 $m^2\ g^{-1}$ for the air treated electrode and to 51.22 $m^2\ g^{-1}$ for the enriched oxygen treated electrode, a 200-fold increase in the surface area. It is noted that the enriched oxygen treated electrode also showed a large increase in hydrophilicity, which may also contribute to the increase in the wetted surface area. Droplets of battery electrolyte were completely absorbed by the electrode, in contrast with the 132° contact angle observed with the untreated electrodes [20]; this increase in hydrophilicity compares similarly to electrodes treated by electrochemical methods [21]. A simplified calculation based on the Butler–Volmer equation shows that a 200-fold increase in surface area can explain the reduced overpotential observed with the treated electrodes. Assuming Tafel behavior for a one electron process, activation overpotential is given by

$$\eta = \frac{RT}{F}\ln\frac{i}{i_0}$$

If it is assumed that the nature of the carbon surface remains the same, the exchange current density, i_0, is constant. The change in overpotential as a result of heat treatment is then

$$\eta_{HT} - \eta_U = \frac{RT}{F}\left(\ln\frac{i_{HT}}{i_0} - \ln\frac{i_U}{i_0}\right) = \frac{RT}{F}\ln\frac{i_{HT}}{i_U}$$

where the subscripts refer to heat treated (HT) and untreated (U) carbon paper. With an assumed 200-fold increase in surface area, the ratio i_{HT}/i_U is equal to 1/200 because the effective current density on the heat treated electrode is reduced by a factor of 200. At 30 °C, the difference in activation overpotentials, $\eta_{HT} - \eta_U$, is ca. −138 mV. While changing the surface area by a factor of 200 may mean that the electrode behavior cannot be described simply by Tafel kinetics, this calculation is reasonable for order of magnitude estimates. Additionally, heat treatment may induce some changes in the surface properties of the carbon fibers, including the addition of oxygen functional groups, which can affect the exchange current density. However, any effect is expected to be relatively minor in comparison with the 200-fold increase in surface area, which alone can account for the observed electrode overpotential change of 140 mV.

Because a large increase in surface area is observed with small changes in the oxygen content on the electrode surface, it is concluded that an increase in the surface area, not an increase in the oxygen content, is predominantly responsible for the enhanced kinetic performance. This observation is a departure from other studies in which enhanced kinetics on treated electrode surfaces are attributed to oxygen functional groups [10–14], but agrees with the findings of Melke et al. [22]. This disparity suggests that the various treatments may have different mechanisms by which they affect the reaction kinetics for carbon felts as compared to carbon papers. Furthermore, this result shows that XPS and other similar techniques that measure changes in the surface chemistry are not sufficient to explain the performance enhancements induced by electrode treatments; the electrochemically wetted surface area is an important factor that must also be considered.

The 400 °C heat treatment in oxygen environments resulted in slight mass loss in the carbon material, up to 7.7% for treatment in enriched oxygen for 45 h. The rate of mass loss was roughly proportional to the amount of oxygen present in the treatment gas and appeared to be linear with respect to time, based on the three time points tested. Nitrogen, air, and enriched oxygen treatments resulted in negligible, 0.10% per hour, and 0.17% per hour mass loss, respectively.

Although the enriched oxygen treatment resulted in a higher wetted surface area than the air treatment, as described above, the electrochemical performance was similar. This suggests that additional kinetic improvements cannot be achieved by further increasing the surface area; there is a maximal surface area that can be utilized. Because a higher oxygen content in the treatment environment results in a higher surface area for the same treatment time, it is possible to reduce treatment time while achieving sufficient surface area by using a higher concentration of oxygen during heat treatment.

3.3. Cycling

Charge/discharge profiles for cycling at 200 mA cm^{-2} are shown in Fig. 2(a). It is noted that the SoC is not the same at the beginning

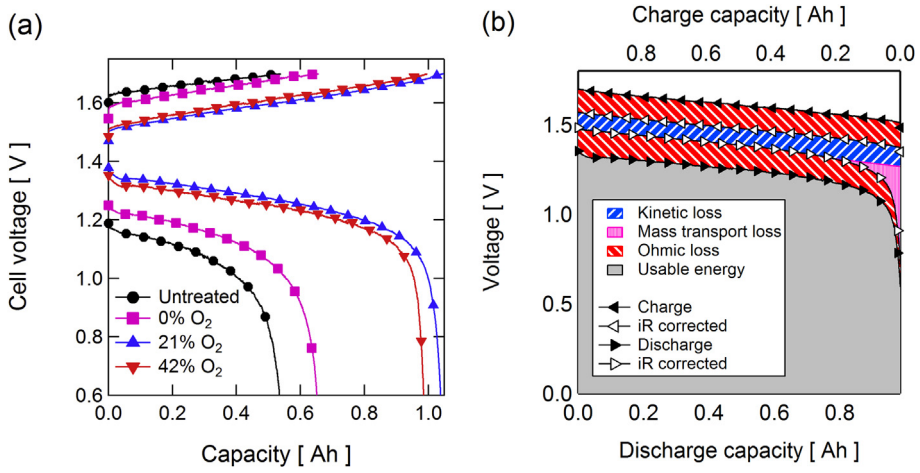

Fig. 2. Charge/discharge profiles obtained at 200 mA cm^{-2} for (a) untreated and 15 h treated samples and (b) 15 h enriched oxygen treated electrode with breakdown of losses from kinetic, ohmic, and mass transport polarizations.

of each discharge profile as a result of differing depths of charge, described in detail later in this section. The improved kinetic performance decreased the charging voltage and increased the discharging voltage, resulting in increased cycling efficiency. Shown in Fig. 2(b) is a graphical representation of losses associated with kinetic, ohmic, and mass transport polarizations for the enriched oxygen treated electrode cycled at 200 mA cm^{-2}. The ohmic loss is found by *iR*-correction of the charge and discharge profiles with the HFR measurements obtained during cycling. The mass transport loss is estimated as the 'tail' region during discharge and is estimated as the deviation from pseudo-linearity present over the majority of the discharge profile. The charge profile remains quasi-linear, indicating relatively minor mass transport loss during charging. The remaining losses are attributed to kinetic polarization. Integration of these curves yields the discharge and charge energies and the energy lost to ohmic and mass transport processes:

$$charge\ energy = \int V_c I_c dt$$

$$discharge\ energy = \int V_d I_d dt$$

$$ohmic\ energy\ loss = \int (V_c - V_{c,iR\ corrected}) I_c dt + \int (V_{d,iR\ corrected} - V_d) I_d dt$$

$$mass\ transport\ energy\ loss = \int \left(V_{d,linear\ extrapolation} - V_{d,iR\ corrected}\right) I_d dt$$

$$coulombic\ efficiency\ (CE) = \frac{\int I_d dt}{\int I_c dt}$$

$$kinetic\ loss = charge\ energy \times CE - discharge\ energy - (ohmic + mass\ transport\ energy\ loss)$$

where I and V refer to the current and voltage, and the subscripts "c" and "d" refer to charge and discharge, respectively. The linear extrapolation used to calculate the mass transport loss is shown in Fig. 2(b). The coulombic energy loss is primarily due to crossover of vanadium ions through the membrane and was ca. 1% for all experiments run, i.e., the coulombic efficiency was ca. 99%.

A summary of these kinetic, ohmic, and mass transport losses as a fraction of the total charge energy is shown in Fig. 3(a) for electrodes cycled at 200 mA cm^{-2}. Kinetic losses were reduced from 20% of the total energy for untreated to 6.0% of the total energy with the enriched oxygen treatment. At 100 mA cm^{-2}, kinetic losses were reduced from 12.5% (untreated) to 3.2% (enriched oxygen treated). The average cell areal specific resistance, taken as the product of the geometric active area and HFR, was measured to be 673.8 ± 45 mΩ cm^2 and resulted in ohmic losses of 14.5–16.5% at 200 mA cm^{-2} and 7.6–8.7% at 100 mA cm^{-2}. The difference in ohmic losses can be attributed to observed variation between cell builds. The mass transport loss was estimated as 1.9% at 200 mA cm^{-2} for the untreated electrodes; the enriched oxygen treated electrodes had a transport loss of 0.9%. At 100 mA cm^{-2}, the mass transport losses were 1.1% (untreated) and 0.6% (enriched oxygen). Since Fig. 1(a) shows that the concentration polarization was similar with all electrodes, this difference in mass transport loss is not a result of improved transport behavior for treated electrodes. Rather, the apparent mass transport difference is attributed to the fact that the raw electrode has a much smaller charge/discharge window, and therefore a larger portion of the charge/discharge curve resides in the mass transport-affected region. Overall, the energy efficiency (non *iR*-corrected) at 200 mA cm^{-2} was increased from 63% to 76% and from 77% to 86% at 100 mA cm^{-2}. This is a significant improvement, especially at these relatively high current densities. It should be noted that, while the energy efficiency could be further improved by selection of a thinner membrane to reduce ohmic losses, the kinetic overpotential in the electrodes was the focus of this study.

In addition to the increased efficiency, treated electrodes enable a deeper charge and discharge window because a lower kinetic overpotential means that a higher SoC can be reached upon charging with the same cutoff voltage. The discharge capacity at 200 mA cm^{-2} was increased from 0.5 Ah for untreated electrodes to 1 Ah with oxygen treated electrodes, which represents an increase from 37% to 74% in the range of SoC that is swept during cycling. The energy discharged was increased from 0.56 Wh (untreated) to 1.21 Wh (enriched oxygen), shown in Fig. 3(b). At

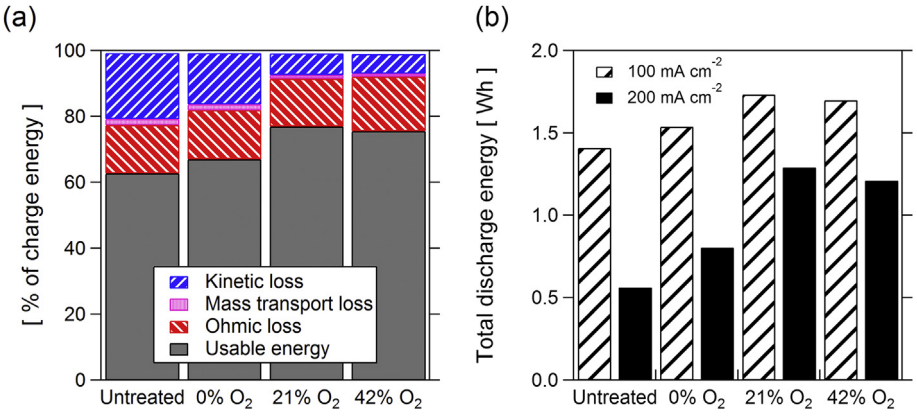

Fig. 3. Summary of cycling for untreated and 15 h treated samples: (a) usable energy and kinetic and ohmic losses at 200 mA cm^{-2} and (b) total discharged energy at 100 mA cm^{-2} and 200 mA cm^{-2}.

100 mA cm^{-2}, gains were less pronounced but still significant, improving the discharge energy from 1.41 Wh (untreated) to 1.70 Wh (enriched oxygen). These results illustrate an important concept: using high performance electrodes can not only reduce stack costs, but also reduce vanadium costs associated with storing a given quantity of energy, especially at higher current densities. Because a larger SoC window is used and higher discharge voltages are achieved, more vanadium is accessible, and the total amount of energy per vanadium is also increased. These results show that the electrolyte cost to store a fixed amount of energy could be cut by 50% for a cell operating at 200 mA cm^{-2} or 17% at 100 mA cm^{-2}. Given that the electrolyte is ca. 40% of the total system capital cost [2], the reduction in vanadium use could be on the order of 5–20% of the total system cost. It should be noted that further increases in the SoC window are possible with advanced design and materials that are the focus of other studies in our laboratory.

4. Conclusions

A high performance carbon paper electrode was developed by heat treating a standard carbon paper in partial oxygen environments. The oxygen concentration of the treatment gas affected the rate of oxidation as well as the final surface area of the treated material. The heat treatment resulted in large surface area enhancements, which explain the reduced activation overpotentials on the order of 140 mV as measured by polarization curves. The increase in surface area, not a change in surface chemistry, can account for the decrease in overpotential. Translated to cycling experiments, heat treating electrodes in an oxygen environment increased energy efficiency from 63% to 76% and more than doubled the usable capacity at a high current density of 200 mA cm^{-2}. Doubling the usable capacity represents an opportunity to decrease system cost by up to 20% by reducing the amount of vanadium necessary to store a given amount of energy.

Acknowledgments

The authors would like to acknowledge Dr. C.-N. Sun for assistance in capacitance measurements, N. Cantillo-Cuello for assistance with BET surface area measurements, and Drs. E.L. Redmond and D.S. Aaron for fruitful discussion. The authors would also like to acknowledge the Office of Naval Research for support of this work under Long Range Broad Agency Announcement (BAA) #N00014-12-1-0887 as well as Tennessee Solar Conversion and Storage using Outreach, Research and Education (TN-SCORE; NSF EPS #1004083). A portion of this work (GMV-XPS) was supported by U.S. Department of Energy's Office of Basic Energy Science (DOE-BES, DE-AC0500OR22725), Division of Materials Sciences and Engineering, under contract with UT-Battelle, LLC.

References

[1] Z. Yang, J. Zhang, M.C.W. Kintner-Meyer, X. Lu, D. Choi, J.P. Lemmon, J. Liu, Electrochemical energy storage for green grid, Chem. Rev. 111 (2011) 3577–3613, http://dx.doi.org/10.1021/cr100290v.
[2] M. Zhang, M. Moore, J.S. Watson, T.A. Zawodzinski, R.M. Counce, Capital cost sensitivity analysis of an all-vanadium redox-flow battery, J. Electrochem. Soc. 159 (2012) A1183–A1188, http://dx.doi.org/10.1149/2.041208jes.
[3] P. Leung, X. Li, C. Ponce de León, L. Berlouis, C.T.J. Low, F.C. Walsh, Progress in redox flow batteries, remaining challenges and their applications in energy storage, RSC Adv. 2 (2012) 10125–10156, http://dx.doi.org/10.1039/c2ra21342g.
[4] X. Li, H. Zhang, Z. Mai, H. Zhang, I. Vankelecom, Ion exchange membranes for vanadium redox flow battery (VRB) applications, Energy Environ. Sci. 4 (2011) 1147–1160, http://dx.doi.org/10.1039/c0ee00770f.
[5] A.Z. Weber, M.M. Mench, J.P. Meyers, P.N. Ross, J.T. Gostick, Q. Liu, Redox flow batteries: a review, J. Appl. Electrochem 41 (2011) 1137–1164, http://dx.doi.org/10.1007/s10800-011-0348-2.
[6] D.S. Aaron, Q. Liu, Z. Tang, G.M. Grim, A.B. Papandrew, A. Turhan, T.A. Zawodzinski, M.M. Mench, Dramatic performance gains in vanadium redox flow batteries through modified cell architecture, J. Power Sources 206 (2012) 450–453, http://dx.doi.org/10.1016/j.jpowsour.2011.12.026.
[7] M.L. Perry, R.M. Darling, R. Zaffou, High Power Density Redox Flow Battery Cells, ECS Trans. 53 (2013) 7–16, http://dx.doi.org/10.1149/05307.0007ecst.
[8] A.J. Bard, L.R. Faulkner, Electrochemical Methods: Fundamentals and Applications, second ed., John Wiley & Sons, Inc., Hoboken, NJ, 2001.
[9] J. Newman, K.E. Thomas-Alyea, Electrochemical Systems, third ed., John Wiley & Sons, Inc., Hoboken, NJ, 2004.
[10] B. Sun, M. Skyllas-Kazacos, Chemical modification of graphite electrode materials for vanadium redox flow battery application—part II. Acid treatments, Electrochim. Acta 37 (1992) 2459–2465, http://dx.doi.org/10.1016/0013-4686(92)87084-D.
[11] L. Yue, W. Li, F. Sun, L. Zhao, L. Xing, Highly hydroxylated carbon fibres as electrode materials of all-vanadium redox flow battery, Carbon 48 (2010) 3079–3090, http://dx.doi.org/10.1016/j.carbon.2010.04.044.
[12] E. Agar, C. Dennison, K. Knehr, E. Kumbur, Identification of performance limiting electrode using asymmetric cell configuration in vanadium redox flow batteries, J. Power Sources 225 (2013) 89–94, http://dx.doi.org/10.1016/j.jpowsour.2012.10.016.
[13] B. Sun, M. Skyllas-Kazacos, Modification of graphite electrode materials for vanadium redox flow battery application—I. Thermal treatment, Electrochim. Acta 37 (1992) 1253–1260, http://dx.doi.org/10.1016/0013-4686(92)85064-R.
[14] C. Flox, M. Skoumal, J. Rubio-Garcia, T. Andreu, J.R. Morante, Strategies for enhancing electrochemical activity of carbon-based electrodes for all-vanadium redox flow batteries, Appl. Energy 109 (2013) 344–351, http://dx.doi.org/10.1016/j.apenergy.2013.02.001.
[15] C.-N. Sun, F.M. Delnick, L. Baggetto, G.M. Veith, T.A. Zawodzinski, Hydrogen evolution at the negative electrode of the all-vanadium redox flow batteries, J. Power Sources 248 (2014) 560–564, http://dx.doi.org/10.1016/j.jpowsour.2013.09.125.
[16] M.M. Mench, Fuel Cell Engines, John Wiley & Sons, Inc., Hoboken, NJ, 2008, http://dx.doi.org/10.1002/9780470209769.
[17] D.S. Aaron, Z. Tang, A.B. Papandrew, T.A. Zawodzinski, Polarization curve

analysis of all-vanadium redox flow batteries, J. Appl. Electrochem. 41 (2011) 1175–1182, http://dx.doi.org/10.1007/s10800-011-0335-7.
[18] J.-S. Lee, T.-J. Kang, Changes in physico-chemical and morphological properties of carbon fiber by surface treatment, Carbon 35 (1997) 209–216, http://dx.doi.org/10.1016/S0008-6223(96)00138-8.
[19] C.U. Pittman, W. Jiang, Z.R. Yue, C.A. Leon y Leon, Surface area and pore size distribution of microporous carbon fibers prepared by electrochemical oxidation, Carbon 37 (1999) 85–96, http://dx.doi.org/10.1016/S0008-6223(98)00190-0.
[20] M.P. Manahan, Q.H. Liu, M.L. Gross, M.M. Mench, Carbon nanoporous layer for reaction location management and performance enhancement in all-vanadium redox flow batteries, J. Power Sources 222 (2013) 498–502, http://dx.doi.org/10.1016/j.jpowsour.2012.08.097.
[21] W. Zhang, J. Xi, Z. Li, H. Zhou, L. Liu, Z. Wu, X. Qiu, Electrochemical activation of graphite felt electrode for VO^{2+}/VO_2^+ redox couple application, Electrochim. Acta 89 (2013) 429–435, http://dx.doi.org/10.1016/j.electacta.2012.11.072.
[22] J. Melke, P. Jakes, J. Langner, L. Riekehr, U. Kunz, Z. Zhao-Karger, A. Nefedov, H. Sezen, C. Wöll, H. Ehrenberg, C. Roth, Carbon materials for the positive electrode in all-vanadium redox flow batteries, Carbon 78 (2014) 220–230, http://dx.doi.org/10.1016/j.carbon.2014.06.075.